Inorganic Materials, Vol. 32, No. 5, 1996, pp. 536–540. Translated from Neorganicheskie Materialy, Vol. 32, No. 5, 1996, pp. 601–606.

Molecular Dynamics Study of Contact Melting in the KCl–KI System

V. S. Znamenskii*, P. F. Zil'berman, P. A. Savintsev*, and E. A. Goncharenko*****

** Kabardino-Balkarian State University, Nal'chik, Russia*

*** Kabardino-Balkarian Agricultural Institute, ul. Tolstogo 185, Nal'chik, 360004 Russia*

**** Design College, Nal'chik, Russia*

Received March 31, 1994; in final form, December 9, 1994

Abstract—Contact melting of KCl–KI ionic crystals was studied by molecular dynamics simulations. Data for determining self-diffusion coefficients as a function of temperature are presented for K^+, Cl^-, and I^-, and exponential-fit parameters are calculated. It is demonstrated that applied electric fields cause changes in radial distribution functions and diffusion coefficients.

INTRODUCTION

Contact melting of ionic crystals is now widely used in both scientific studies and technological applications. The nature and mechanisms of this phenomenon were investigated extensively [1–5] to reveal ways of controlling the major parameters of the process. In most works, however, contact melting was studied experimentally, or only its macroscopic aspects were considered.

With the advent of computer simulation techniques, microscopic approaches to studying the kinetic and structural features of this nonequilibrium process became possible. In molecular dynamics (MD) simulations [6,7], Newton's equations of motion are integrated to obtain the coordinates and velocity of each ion. Subsequent statistical treatment of these results yields both thermodynamic and structural parameters of the system.

MOLECULAR DYNAMICS SIMULATION

We used MD simulations to model contact melting of KCl–KI crystals. The system included 54 Cl^-, 108 K^+, and 54 I^- ions enclosed in a cubic simulation box whose size, L = 2.968 nm, was found from the corresponding pair potential to fit to the ion dimensions (Table 1). We used Fumi–Tosi potential functions

$$V(r_{ij}) = \mathrm{sgn}(q_i q_j)\frac{e^2}{4\pi\varepsilon_0 r_{ij}} + B_{ij}\exp(-\alpha_{ij} r_{ij}) - \frac{C_{ij}}{r_{ij}^6} - \frac{D_{ij}}{r_{ij}^8},$$

where $B_{ij} = \beta_{ij} b \exp[\alpha_{ij}(\sigma_i + \sigma_j)]$, $b = 3.38 \times 10^{-20}$ J.

The parameters of the pair potential are summarized in Table 2. The time step used in all simulations was 1.09×10^{-14} s. Periodic boundary conditions were employed; at each time step, the system was relaxed to thermal equilibrium. The equations of motion were integrated using the leapfrog centered difference algorithm.

The software used allowed us to display ion trajectories as well as structural and kinetic characteristics of the system.

ACCURACY OF MOLECULAR DYNAMICS SIMULATIONS

We estimated both systematic errors, by comparing simulation results with experimental data, and random errors (fluctuations), by varying initial velocities in repeat simulations. As the temperature was raised

Table 1. Ionic masses and effective sizes used in simulations

Ion	K^+	Cl^-	I^-
$m \times 10^{27}$, kg	64.7	58.872	210.733
$\sigma \times 10^{10}$, m	1.463	1.585	1.907

Table 2. Parameters of the Fumi–Tosi potential

Ionic pairs	$C \times 10^{25}$, J nm^6	$D \times 10^{27}$, J nm^8	β_{ij}	α_{ij}, nm^{-1}
Cl^-–Cl^-	124.5	250.0	0.75	2.967
Cl^-–K^+	48.0	73.0	1	2.96
K^+–K^+	24.3	24.0	1.25	2.892
Cl^-–I^-	263.75	690	0.75	2.892
K^+–I^-	82.0	156.0	1	2.817
I^-–I^-	403.0	1130.0	0.75	2.817

0020-1685/96/3205-0536$15.00

starting just above the melting point, the diffusion coefficients and their fluctuations increased, whereas the relative fluctuations decreased from 30% at 1000 K to 14–17% at 1500 K.

The relative errors in the temporal characteristics of the velocity autocorrelation function were about 2% for the first zero crossing and 4% for the first minimum; subsequently, the error increased. The relative error in the parameters of the partial radial distribution functions did not exceed 7%.

DIFFUSION COEFFICIENTS

Simulations of trajectories as a function of temperature for ions diffusing both within and beyond the contact zone showed that the mobility of ions is substantially higher at the interface than in the bulk. This difference is especially pronounced in the vicinity of the contact-melting temperature. A further increase in temperature is accompanied by a sharp increase in the diffusion coefficient and the formation of interfacial ion microgroups. These microgroups are responsible for subsequent formation of the liquid phase, accompanied by marked structural changes. According to our simulations, nucleation time may be of order 10^{-11} s.

The diffusion coefficients were determined by analyzing the simulation results, using the relation

$$Q_k(t) = \frac{1}{N_k}\sum_{i \in P_k}(R_i(t_0 + t) - R_i(t_0)^2) = 6tD_k + C_k,$$

$$t_1 < t < t_2,$$

where Q_k is the rms displacement for ionic species k, N_k is the number of ions of species k, R_i is the position vector of ion i, P_k is the set of numbers of species k, t_0 is the point in time at which two ionic systems are brought in contact, t_1 and t_2 bound a time interval within which the $Q_k(t)$ dependences can be considered linear, and C_k are constants.

We obtained the following expressions for the partial diffusion coefficients as a function of temperature:

$$D_{K_I} = 0.573785\exp[-21.863/(kT)],$$

$$D_{K_{Cl}} = 0.687254\exp[-20.1607/(kT)],$$

$$D_{Cl_{Cl}} = 0.848843\exp[-21.728/(kT)],$$

$$D_{I_{Cl}} = 1.34446\exp[-31.1539/(kT)],$$

where D_{K_I}, $D_{K_{Cl}}$, $D_{Cl_{Cl}}$, and $D_{I_{Cl}}$ are the self-diffusion coefficients for the K^+ ions surrounded by I^- ions and the K^+, Cl^-, and I^- ions surrounded by Cl^- ions, respectively. As follows from these data, $D_{K_{Cl}}$ is larger than D_{K_I}.

The effect of dc electric field E was taken into account by adding a force acting on each ion according to its charge. Simulations carried out for different

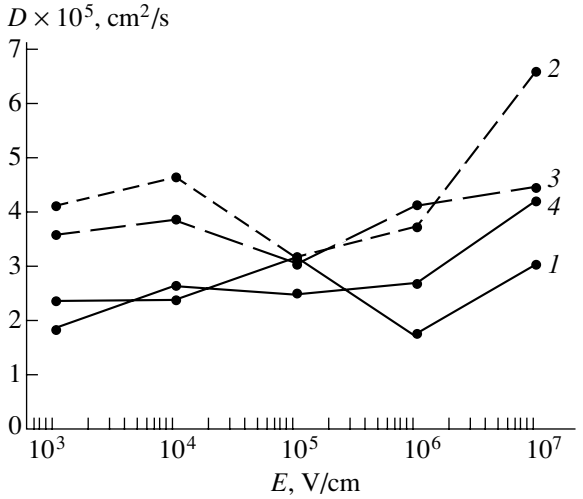

Fig. 1. Partial self-diffusion coefficients as a function of applied electric field for the KCl–KI system: (*1*) Cl^-, (*2*) I^-, (*3*) K^+ in KCl, (*4*) K^+ in KI.

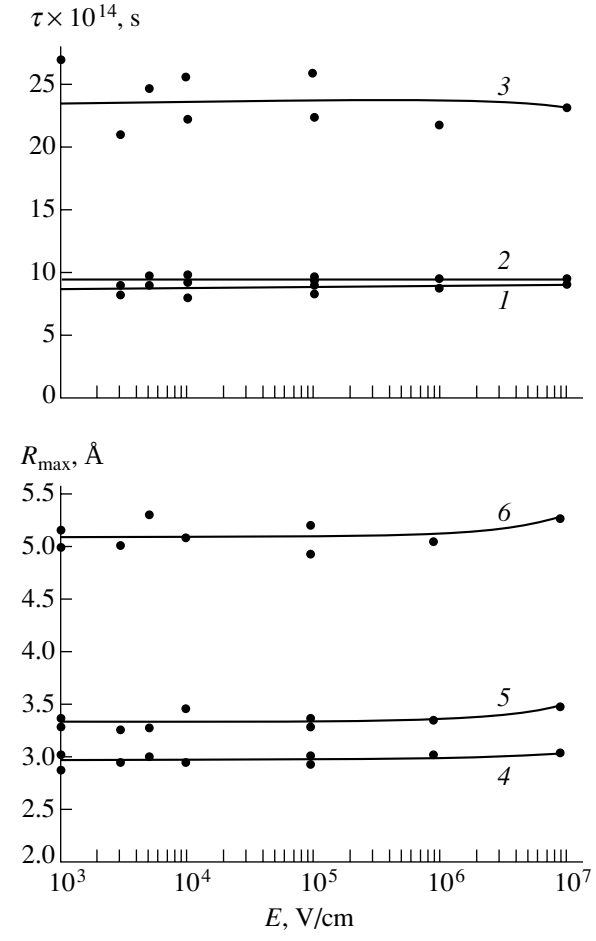

Fig. 2. Electric-field dependences of the velocity autocorrelation function and partial distribution functions for the KCl–KI system: (*1*) Cl^-, (*2*) K^+, (*3*) I^-, (*4*) Cl^-–K^+, (*5*) I^-–K^+, (*6*) I^-–I^-.

Table 3. Parameters of the velocity autocorrelation function at different electric-field intensities

Ion	$\tau_0 \times 10^{14}$, s	$\tau_{min} \times 10^{14}$, s	z_{min}	$\tau_{max} \times 10^{14}$, s	z_{max}
		$E = 0$			
K^+	9.2	15.1	−0.250	−0.04	28.8
Cl^-	8.6	11.3	−0.175	−0.07	20.4
I^-	21.3	–	–	–	–
		$E = 10^4$ V/cm			
K^+	9.2	14.9	0.25	31.2	0.04
Cl^-	8.0	12.9	0.20	23.5	0.07
I^-	22	–	–	–	–
		$E = 10^7$ V/cm			
K^+	19.2	35.0	0.20	–	–
Cl^-	5.8	11.2	0.24	30.0	0
I^-	5.7	0.22	9.8	42.2	0.04

values of E showed that the general trend is toward an increase in partial diffusion coefficients with increasing E. At the same time, each ionic species exhibits its own features In the range 10–100 V/cm, the diffusion coefficient of K+ decreases, while those of the other ions increase. Starting at E = 1 kV/cm, the $D = f(E)$ curves exhibit notable variations for all of ionic species (Fig. 1). The simulated data are in reasonable agreement with reported measurements [8, 9].

CONTACT-MELTING TEMPERATURE

The contact-melting temperature T_m, as assessed from the variation of the diffusion coefficient, is 675 K. The temperature dependence of the diffusion coefficient was fitted to a straight line at temperatures well above T_m, and T_m was determined as the intercept on the D = 0 axis. Calculations with the Fumi–Tosi potential yield T_m = 603 K, in close agreement with experiment [10].

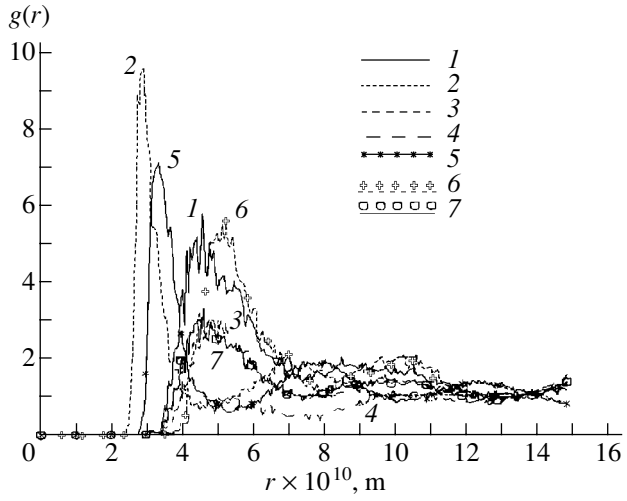

Fig. 3. Partial radial distribution functions for the KCl–KI system at T = 920 K and E = 0: (*1*) Cl^-–Cl^-, (*2*) Cl^-–K^+, (*3*) K^+–K^+, (*4*) I^-–Cl^-, (*5*) I^-–K^+, (*6*) I^-–I^-, (*7*) K^+–Cl^- (I^-).

VELOCITY AUTOCORRELATION FUNCTION

The velocity autocorrelation function

$$z(t) = \langle V(0)V(t)\rangle m/3kT$$

(were m, is the particle mass) obtained for the system under study is typical of ionic systems. With increasing simulation temperature, the time until the first zero crossing increases, whereas the oscillation period drops. Given that the velocity autocorrelation function characterizes the rate at which the velocities of the ions vary as a result of interaction, it may be concluded that this rate decreases as a function of increasing temperature. The major parameters of the velocity autocorrelation function are roughly constant in low electric fields (Fig. 2) and change sharply in the vicinity of the breakdown field (Table 3).

PARTIAL RADIAL DISTRIBUTION FUNCTIONS

In describing the melt structure and its variation as a function of field and temperature, a large body of information is provided by partial radial-distribution functions (PRDFs), which were calculated here by the relation

$$g_{ab}(r) = \frac{V}{N_b}\frac{n_b(r)}{4\pi r^2},$$

where g_{ab} is the partial distribution function for particles b around particles a, V is the volume of the simulation box, N_b is the number of particles of species b, $n_b(r)\Delta r$ is the number of particles b within a spherical zone of thickness Δr at distance r from particle a, and r is the distance between particles a and b.

The PRDFs calculated for the system under consideration are typical of ionic melts (Fig. 3) and vary insignificantly as a function of temperature (Table 4).

Analysis of our results shows that the long-range order degrades starting at the contact-melting temperature. The next-nearest-neighbor-distance distribution is notably broadened, although the width of the first RDF peak provides evidence that the short-range order persists for at least 1.3×10^{-11} s. This averaging time is much longer than the time it takes an ion to travel the interionic distance, indicative that the melt is in a quasicrystalline state.

With increasing temperature, the position of the first nonzero value shifts toward smaller distances. A similar, although notably smaller, shift would be produced by an electric field. The position of the first peak (R_{max}) characterizes the nearest-neighbor distance. As follows from Fig. 4, this distance also depends on simulation temperature: with increasing temperature, it is nearly

Table 4. Parameters of the radial distribution function for the KCl–KI system

T, K	$r_0 \times 10^{10}$, m	$r_{max} \times 10^{10}$, m	$g(r_{max})$	$r_0 \times 10^{10}$, m	$r_{max} \times 10^{10}$, m	$g(r_{max})$
	K^+–Cl^-			K^+–I^-		
920	2.4	3.0	8.6	2.7	3.4	6.9
1020	2.3	3.0	8.2	2.6	3.4	7.3
1120	2.4	3.0	8.0	2.6	3.4	6.4
1220	2.4	3.0	7.8	2.7	3.3	5.8
1320	2.4	2.9	7.7	2.7	3.3	5.7
1420	2.4	2.9	7.6	2.8	3.3	5.7
1520	2.3	2.9	7.6	2.5	3.4	5.4
1620	2.4	2.8	8.0	2.6	3.4	5.2

constant or rises for oppositely charged ions and decreases for ions of the same charge. In addition, both the first and the second PRDF peaks broaden with increasing temperature.

Our results agree well with x-ray scattering data [11]. Electric fields cause an insignificant shift of the first peak (Fig. 2). The most pronounced effect was observed for the I^-–I^- ions. The first peaks are asymmetric, with a steeper slope on the smaller *r*-value side. This observation suggests that the nearest-neighbor ions in the melt are in "rigid" contact. The second peaks are much broader than the first; accordingly, their position was determined with notably lower accuracy. For the K^+–Cl^- and K^+–I^- pairs, the ratio of the peak heights is 1.385. As the temperature is raised, this ratio decreases to 1.315. The peak height for the I^-–I^- pairs is 1.1 times greater than that for the Cl^-–Cl^- pairs and 2.235 times greater than for the K^+–K^+ pairs. At the same time, the first peaks are more than 1.5 times stronger than the second peaks. Analysis of peak heights shows that the strongest interaction occurs between the K^+ and Cl^- ions.

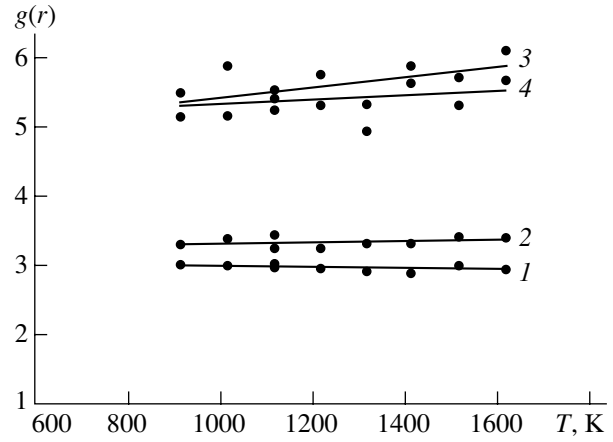

Fig. 4. Position of the first PPDF peaks as a function of temperature for the KCl–KI system: (*1*) Cl^-–K^+, (*2*) K^+–I^-, (*3*) I^-–I^-, (*4*) K^+–K^+.

An increase in temperature is accompanied by a decrease in peak height for all of the pairs. Weak electric fields, under 1 kV/cm, also lower the peaks. The peak heights decrease by a factor of 1.01, 1.06, 1.09, and 1.35 for the K^+–Cl^-, K^+–I^-, Cl^-–Cl^-, and K^+–K^+ pairs, respectively. As field intensity is raised from 1 to 10 kV/cm, peak heights increase by a factor of 1.05, 1.4, 1.29, and 1.14 for the K^+–Cl^-, K^+–I^-, I^-–I^-, and K^+–K^+ pairs, respectively. For the Cl^-–Cl^- pairs, the peak height continues to decrease.

Note that the PRDF peaks are much stronger for the crystal than for the melt. The coordination number for the K^+–Cl^- pairs at 920 K was calculated to be 3.6, in agreement with experimental data.

CONCLUSION

Contact melting in the KCl–KI system was studied by molecular dynamics simulation. Structural and diffusion parameters of the melt are calculated as a function of temperature and applied electric field, and the contact-melting temperature is evaluated.

REFERENCES

1. Savintsev, P.A. and Avericheva, V.E., Contact Melting of Crystals, *Izv. Vyssh. Uchebn. Zaved., Fiz.*, 1957, no. 1, p. 162.
2. Zil'berman, P.F. and Savintsev, P.A., Contact Melting in Crystals of Alkali Halides, *Neorg. Mater.*, 1992, vol. 28, no. 3, pp. 614–618.
3. Zil'berman, P. and Savintsev, P., The Contact Melting As the Method of Investigation of Diffusion Processes in Melting Salts, *III Int. Symp. on Molten Salt Chemistry and Technology*, Paris, 1991, p. 63.
4. Hockney, R.W. and Eastwood, J.W., *Computer Simulation Using Particles*, New York: McGraw-Hill, 1984.
5. Znamenskii, V.S., Savintsev, P.A., and Zil'berman, P.F., Molecular Dynamics Study of the Contact Melting

Method, *Zh. Fiz. Khim.*, 1993, vol. 67, no. 7, pp. 1504–1507.

6. Znamenskii, V.S., Savintsev, P.A., Zil'berman, P.F., and Savintsev, A.P., Parameters of Contact Melting in Ionic Systems: Molecular Dynamics Simulations with Pauling and Fumi–Tosi Potentials, *Neorg. Mater.*, 1994, vol. 30, no. 4, pp. 514–516.
7. Sangster, M.J.L. and Dixon, M., Interionic Potentials in Alkali Halides and Their Use in Simulation of Molten Salts, *Adv. Phys.*, 1976, vol. 25, no. 3, pp. 247–342.
8. Zil'berman, P. and Savintsev, P., *The Lars Onsader Symp.*, Norway, Paris, 1993, p. 128.
9. Zil'berman, P.F. and Savintsev, P.A., Contact Melting in the KNO_3–Na_2CO_3 System, *Zh. Fiz. Khim.*, 1992, vol. 66, no. 2, pp. 521–525.
10. Zil'berman, P.F., Contact Melting in Ionic Crystals, *Doctoral (Phys.–Math.) Dissertation*, Tomsk: Inst. of Strength Physics and Materials Research, 1993.
11. Bloom, H. and Bockris, J.O.M., The Structure of Ionic Liquids, *Fused Salts*, Sundheim, B.R., Ed., New York: McGraw-Hill, 1964.